THE JOURNAL OF BIOLOGICAL CHEMISTRY
Vol. 274, No. 36, Issue of September 3, pp. 25317–25329, 1999

Printed in U.S.A.

Heparin Dodecasaccharide Binding to Platelet Factor-4 and Growth-related Protein-α

INDUCTION OF A PARTIALLY FOLDED STATE AND IMPLICATIONS FOR HEPARIN-INDUCED THROMBOCYTOPENIA*

(Received for publication, December 23, 1998, and in revised form, May 28, 1999)

Dmitri Mikhailov‡, Helen C. Young‡, Robert J. Linhardt§, and Kevin H. Mayo‡¶

From the ‡Department of Biochemistry, Molecular Biology & Biophysics, Biomedical Engineering Center, University of Minnesota Health Science Center, Minneapolis, Minnesota 55455 and the §Division of Medicinal and Natural Products Chemistry and Department of Chemical and Biochemical Engineering, University of Iowa, Iowa City, Iowa 52242

α-Chemokines are known heparin-binding proteins. Here, a heparin dodecasaccharide (H12) was purified and used in NMR studies to investigate binding to growth-related protein-α (Gro-α) and to platelet factor-4-M2 (PF4-M2), an N-terminal chimera of PF4. Pulsed field gradient NMR was used to derive diffusion coefficients as the protein (monomer):H12 ratio was varied. In the absence of H12, both PF4-M2 and Gro-α give diffusion coefficients consistent with the presence of mostly dimers. As the PF4-M2:H12 ratio is increased from 1:6 to 2:1, the diffusion coefficient increases, indicating dissociation to the monomer state. On addition of H12 to either protein, $^{15}N/^{1}H$ heteronuclear single quantum coherence NMR data demonstrate loss of ^{1}H resonance dispersion and intensity, particularly at protein:H12 ratios of 2:1 to 4:1, indicating significant perturbation to native structures. For Gro-α in particular, ^{1}H resonance dispersion appears random coil-like. At these same ratios, circular dichroism (CD) data show general retention of secondary structure elements with a slight shift to additional helix formation. Random coil NMR resonance dispersion suggests a shift to a less compact, partially folded, and/or more flexible state. Further addition of H12 causes resonance intensity and dispersion to return making NMR spectra appear native-like. At low PF4-M2:H12 ratios, loss of resonance intensity for residues proximal to Arg-20 and Arg-22 in three-dimensional NMR HCCH-TOCSY spectra suggests that the Arg-20-Arg-22 loop either interacts most strongly with H12 and/or that binding at this site is heterogeneous. This domain was previously shown to be crucial to heparin binding. Of particular interest to the biology of PF4-heparin complex formation, heparin-induced thrombocytopenia antibody binding occurs at about the same PF4-M2:H12 ratio as does this transition to a partially folded PF4-M2 state, strongly suggesting that heparin-induced thrombocytopenia antibody recognizes a less folded, lower aggregate state of the protein.

Heparin is a polydisperse, sulfated copolymer of 1–4-linked glucosamine and uronic acid residues. Most of the heparin molecule is accounted for by this repeating disaccharide unit, which consists primarily of 2-*O*-sulfated-α-L-idopyranosyluronic acid 2-sulfate and 2-deoxy-2-sulfamido-α-D-glucopyranose ($GlcNSO_3$) 6-sulfate (1). Fig. 1 illustrates the covalent structure of a heparin dodecasaccharide. A number of proteins have been identified that bind avidly to polyanionic heparin and heparin-derived polysaccharides, *e.g.* fibroblast growth factor-2 (FGF-2)[1] (2), hepatocyte growth factor (3), antithrombin-III (4), and α-chemokines (5) like platelet factor-4 (PF4) and growth-related protein-α (Gro-α). α-Chemokines, which demonstrate a variety of physiological activities, some of which may be related to binding heparin-like glycosaminoglycans on the surface of cells, present good model systems for exploring heparin-protein interactions. PF4 is perhaps the strongest heparin-binding protein known (6). During coagulation, for example, PF4 displaces thrombin from heparin, where it forms anticoagulant complex with antithrombin-III, into solution, where thrombin is procoagulant through its interactions with blood clotting factors (7). PF4 exhibits other physiological effects (5), including stimulation of fibroblast attachment to the substrate, chemotactic activity with respect to neutrophils, monocytes and fibroblasts, potentiation of platelet aggregation and inhibition of megakaryocytopoiesis, angiogenesis, and solid tumor growth. Gro-α (also called melanoma growth stimulatory activity (MGSA)) is secreted by a number of different cells and demonstrates a variety of biological activities (5), including stimulation of melanoma cell growth, neutrophil chemotaxis, and inhibition of collagen expression.

α-Chemokines can exist as dimers or tetramers (5). In solution, PF4 may form dimers and tetramers, whereas Gro-α and interleukin-8 (IL-8) are observed to aggregate only to the dimer state. Structure analysis of native human PF4 (8) indicates that each subunit (A, B, C, and D) of the tetramer has a three-stranded β-sheet scaffold onto which is folded an amphipathic C-terminal α-helix and an aperiodic N-terminal segment. In general, such tetrameric structures naturally have three types of monomer-monomer (dimer) interactions, which are referred to in the literature as AB, AC and AD. In AB-type dimers, monomers associate by continuing their anti-parallel

* This work was supported by Grant AHA-96006050 from the American Heart Association and National Institutes of Health Grants GM38060 and HL52622 and benefited from the use of the high field NMR facility at the University of Minnesota. The costs of publication of this article were defrayed in part by the payment of page charges. This article must therefore be hereby marked "*advertisement*" in accordance with 18 U.S.C. Section 1734 solely to indicate this fact.

¶ To whom correspondence should be addressed: Dept. of Biochemistry, Biomedical Engineering Center, 4-225 Millard Hall, University of Minnesota Health Science Center, 435 Delaware St. S.E., Minneapolis, MN 55455.

[1] The abbreviations used are: FGF, fibroblast growth factor; NOE, nuclear Overhauser effect; NOESY, two-dimensional NMR nuclear Overhauser effect spectroscopy; HSQC, heteronuclear single quantum coherence; HCCH-TOCSY, three-dimensional ^{1}H-^{13}C-^{13}C-^{1}H total correlated spectroscopy; GAG, glycosaminoglycan; PF4, platelet factor-4; PF4-M2, N-terminal chimera of PF4; IL-8, interleukin-8; Gro-α, growth-related protein-α; HPLC, high performance liquid chromatography; H12, heparin dodecasaccharide; HITT, heparin-induced thrombocytopenia/thrombosis.

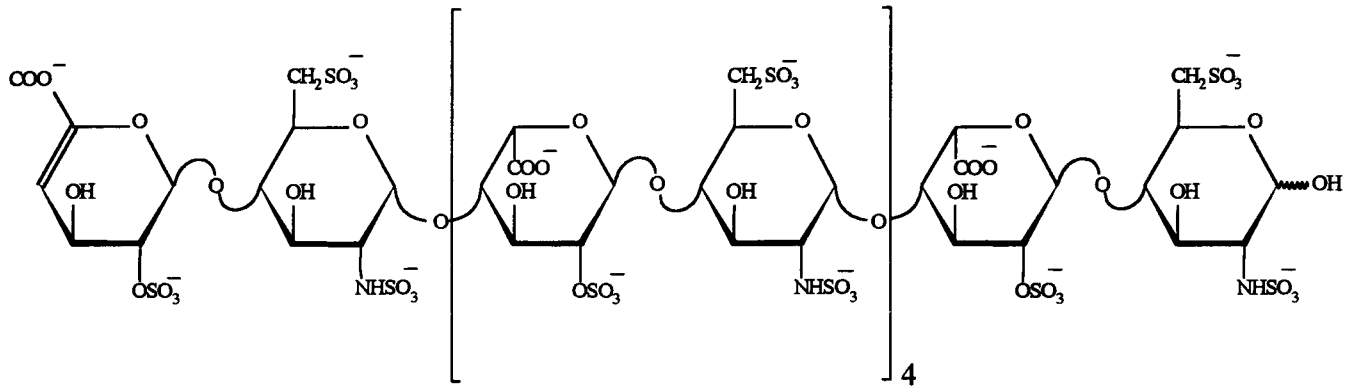

FIG. 1. **Covalent structure of heparin-derived dodecasaccharide.**

β-sheets to form a six stranded sheet. Gro-α and IL-8 associate as AB-type dimers. The general AB-type dimer fold that is observed in all α-chemokines is illustrated in Fig. 2 for PF4 and Gro-α. In the crystal (8), as well as in solution (9), native PF4 AB-type dimers associate to form tetramers that are asymmetric, *i.e.* each monomer in the tetramer has a slightly different orientation with respect to any other monomer subunit. In NMR spectra, this gives rise to multiple sets of resonances for each residue, one set from each subunit, making NMR solution studies with native PF4 intractable. Substitution of a highly acidic N-terminal region of PF4 with the N-terminal sequence of homologous IL-8 results in formation of a symmetric tetramer (9) wherein each monomer is identically positioned within the tetramer, thus facilitating interpretation of NMR experiments. This chimera, named PF4-M2, binds heparin nearly as tightly as native PF4 (9) and has been used in the present heparin binding studies.

The C terminus of PF4 (. . . $LY^{60}KKIIK^{65}KLLES^{70}$) (and of α-chemokines in general) was proposed originally to be the primary mediator of heparin binding (10, 11), particularly via interactions with the four lysine residues conformed spatially *in tandem* on the solvent-exposed surface of the C-terminal α-helix. In fact, a single amino acid replacement of Lys-65 (PF4) by Glu-63 (Gro-α) (. . . $IVKKIIE^{63}KMLNSDKS$) was used to rationalize heparin binding differences between these two proteins (6). Analysis of the PF4 tetrameric structure, however, reveals the presence of a ring of positive charge circumventing the molecule and running perpendicular to the C-terminal helices (8, 9). No experimentally determined structure of the PF4-heparin complex is yet known. However, two models for heparin binding to PF4 have been devised in which the heparin molecule binds either parallel (11) or perpendicular (12) to the C-terminal α-helixes of the AB dimer (see Fig. 2). In an experimental NMR study, Mayo *et al.* (13) deduced that the perpendicular binding mode is most probably favored and that, even though heparin (9,000-dalton cut-off) interacted with residues within the ring of positively charged groups, Arg-20 and Arg-22 were crucial to the binding process, more so than the C-terminal lysines.

These and most other protein-heparin binding studies have been performed using commercial preparations of heparin that result in limited structural information due to heterogeneity of the heparin polymer. Moreover, these heparin preparations are known to induce protein precipitation when the heparin:protein ratio is less than about 3:1. One way to avoid these problems is to use heparinase-derived, homogeneous preparations of short-chain heparins. Heparin chains up to tetradecasaccharide in length can be obtained (14); however, for milligram quantities required for NMR studies, a dodecasaccharide is probably the best attainable. The present study, therefore, is aimed at investigating interactions of a heparin-derived dodecasaccharide (H12) (Fig. 1) with PF4-M2 and Gro-α.

MATERIALS AND METHODS

Heparin Dodecasaccharide Isolation—Approximately 2 g of heparin was dissolved in 100 ml of distilled water and dialyzed exhaustively, freeze-dried, and prepared at exactly 20 mg/ml in distilled water (15). To 50 ml of heparin (20 mg/ml) was added 450 ml of sodium phosphate buffer (55 mM sodium phosphate, pH 7) containing 800 mIU of heparinase. The reaction mixture was incubated at 30 °C for 20 h. At 30% reaction completion, reaction was terminated by heating to 100 °C. The depolymerization mixture was separated, and individual low molecular weight heparin oligosaccharide fractions were isolated by gel permeation chromatography and strong-anion exchange HPLC as discussed previously (14). The heparin oligosaccharide used in the present study is a dodecasaccharide with the structure shown in Fig. 1. In the present report, this heparin-derived dodecasaccharide is referred to as H12. This procedure produced milligram quantities of H12 necessary for the NMR studies; nonetheless, amounts of H12 were limited to about 4 mg.

Isolation of Recombinant PF4-M2 and Gro-α—Synthetic genes for PF4-M2 and Gro-α were expressed as non-fusion proteins in *Escherichia coli* BL21 cells and grown at the 10-liter scale with ^{15}N-enriched ammonia as the nitrogen source and [^{13}C]glucose as the carbon source (9). Proteins were purified and refolded essentially as described previously (16). Purity was assessed by Coomassie staining of SDS-polyacrylamide gel electrophoresis, analytical C4 reverse phase HPLC, and amino acid analysis. Typically, several hundred milligrams of greater than 95% pure material was isolated from 100 g of starting material. Protein concentration was determined by using the bicinchoninic acid (BCA) assay (17) and calculated on the basis of protein concentrations obtained from a standard dilution series of bovine serum albumin. Protein concentrations also were checked by using the methods of Lowry *et al.* (18) and of Waddell (19).

PF4-M2 and Gro-α Sample Preparation—$^{15}N/^{13}C$-labeled PF4-M2 was dissolved in 10%/90% D_2O/H_2O at a concentration of 6 mg/ml, pH 5.9, 20 mM NaCl. This PF4-M2 solution was then titrated into a solution of H12 in aliquots of 30 μl to reach the following PF4-M2 (monomeric): H12 ratios: 1:6, 1:3, 1:2, 1:1, 2:1, and 4:1. To achieve the final ratio, unlabeled PF4-M2 was added to the 2:1 mixture of $^{15}N/^{13}C$-labeled PF4-M2 and H12. The addition of each aliquot of PF4-M2 solution induced some opacity to the H12 solution, which became clear after heating up to 50 °C for about 30 min or sitting overnight at room temperature. Following mixing of H12 and PF4-M2, the solution pH remained essentially unchanged, varying by no more than 0.05 pH units.

^{15}N-Labeled Gro-α was dissolved in 10%/90% D_2O/H_2O at concentration of 10 mg/ml. In order to facilitate NMR assignments, the solution pH was adjusted to 5.7 to be the same as that used in the assignment/structural studies of Fairbrother *et al.* (20). To this solution of Gro-α was added microliter aliquots of a concentrated solution of H12 to achieve the following Gro-α (monomeric):H12 ratios: 20:1, 10:1, 4:1, 2:1, and 1:1. Addition of the initial H12 aliquot to the protein solution induced some opacity to the solution which, as with PF4-M2, became clear after heating to 50 °C for 30 min or allowing it to stand overnight at room temperature. When the Gro-α:H12 ratio reached 4:1 or greater, addition of more H12 induced no further cloudiness.

NMR Experiments—Two-dimensional and three-dimensional NMR spectra were collected on a Varian Inova 600 spectrometer. H12 ^1H

resonances were assigned by using a combination of TOCSY (21) (2048 × 256, 60-ms mixing time) and NOESY (22, 23) (2048 × 256, 100-ms mixing time) experiments performed at 30 °C and at 50 °C. NMR results were similar to those reported previously by Pervin *et al.* (14). In these two-dimensional NMR experiments, suppression of the water resonance was carried out using the WATERGATE sequence (24). Two-dimensional NMR ^{15}N gradient-enhanced HSQC (25) (2048 × 256) spectra were collected at various molar ratios of protein:H12 as noted above. The transmitter offset for the ^{1}H dimension was set on the water resonance. The water signal was suppressed by applying selectively shaped pulses. Two-dimensional NMR data were processed off line using the programs Felix (Biosym/MSI, San Diego) and VNMR (Varian) by zero-filling to achieve 1024 × 1024 real data points and by using skewed-sinebell or Gaussian window functions.

HCCH-TOCSY (26) (64 × 48 × 1024, 15.6 ms mixing time) three-dimensional NMR experiments were acquired at 50 °C and were used to assign PF4-M2 side-chain resonances for the protein in the absence and in the presence of approximately 5-fold molar heparin excess. Previous ^{1}H resonance assignments were used from data acquired on pure PF4-M2 (9). Assignments for the mixture were made under the assumption that ^{13}C chemical shifts for side-chain carbons were nearly the same in both PF4-M2 free and H12-bound states.

Gradient-enhanced TOCSY-HSQC (27, 28) (64 × 48 × 1024, 60-ms mixing time) three-dimensional NMR experiments were performed at 30 °C in order to complete ^{15}N assignments of Gro-α. ^{1}H and ^{15}N chemical shifts for Gro-α were essentially the same as those reported previously by Fairbrother *et al.* (20). The raw three-dimensional NMR data were zero-filled to 256 × 256 × 1024 and multiplied by a sinebell window function using VNMR software (Varian).

Translational diffusion measurements were performed on a Varian Inova 500 NMR spectrometer by using the pulse field gradient (PFG) method as described previously (29). Similar PFG-NMR studies have been done to assess the self-association and complexation of other protein systems (*e.g.* 30). The PFG longitudinal Eddy current delay pulse sequence (31) was used for all diffusion measurements. For unrestricted molecular diffusion in an isotropic medium, the amplitude of the NMR signal, A, normalized to the signal obtained in the absence of gradient pulses is related to the diffusion coefficient D by Equation 1.

$$A(g^2) = A(0)\exp[-\gamma^2 g^2 \delta^2 D(\Delta - \delta/3)] \quad \text{(Eq. 1)}$$

γ is the gyromagnetic ratio for the observed nucleus (^{1}H in this case); g and δ are the magnitude and duration of the magnetic field gradient pulses, respectively, and Δ is the time between gradient pulses. Gradient strength was calibrated based on the known diffusion constant of water (2.3×10^{-5} cm^2/s at 25 °C). Other parameters in Equation 1 were set as follows: δ = 4 ms, Δ = 34.2 ms. For each measurement, 11 NMR spectra were collected for different values of g and processed off-line by using a home-written VNMR macro.

Diffusion constants for PF4-M2 and Gro-α were measured over a range of temperatures from 10 °C to 60 °C. Diffusion measurements of solutions of PF4 (30 mg/ml) and IL-8 (10 mg/ml) were used as references for tetramer and dimer sizes, respectively. The Stokes-Einstein equation,

$$D = k_B T/6\pi\eta R, \quad \text{(Eq. 2)}$$

where R is the macromolecular radius and η is the solution viscosity, was used to relate D to the apparent molecular weight M_{app}. The apparent molecular weight for globular proteins is proportional to R^3, whereas for random coils, it is proportional to R^2 (32). From Equation 2, it follows that under the same conditions, diffusion coefficients for two different proteins related by their apparent molecular weights is shown by Equation 3.

$$(D1/D2) = (M2_{app}/M1_{app})^a \quad \text{(Eq. 3)}$$

Here, the superscript a is 1/3 for compact proteins and 1/2 for random coils. According to this equation, a factor of 2 difference in molecular weights (*e.g.* monomer to dimer) results in a $D1/D2$ ratio of 1.26 to 1.41. This relationship, of course, is an approximation and works best for monomeric proteins having a spherical shape. The actual molecular shape and configuration of the aggregate are expected to affect the diffusion coefficient. Thus, using apparent molecular weights rather than experimentally measured diffusion coefficients can be a source of error. Therefore, these results are presented here in terms of diffusion coefficients.

Circular Dichroism—Circular dichroic (CD) spectra were measured on a Jasco JA-710 automatic recording spectropolarimeter coupled to a data processor. Curves were recorded digitally and fed through the data processor for signal averaging and base-line subtraction. Spectra were recorded at 30 °C in the presence of 10 mM potassium phosphate, over a 190–250-nm range using a 0.5-mm path length, thermally jacketed quartz cuvette. Temperature was controlled by using a NesLab water bath. Protein concentration was 0.03 mM. The scan speed was 20 nm/min. Spectra were signal-averaged eight times, and an equally signal-averaged solvent base line was subtracted. CD spectra were deconvoluted as described by Sreerama and Woody (33).

RESULTS

Since α-chemokines PF4-M2 and Gro-α are known to bind heparin and heparin fragments relatively tightly (6, 9), it was thought that mixing pure H12 and pure PF4-M2 or Gro-α would produce a complex of protein and GAG whose NMR spectral features would be similar to the sum of the individual species. The situation turned out to be not so simple, and the following sections report observations from diffusion, NMR, and CD measurements which catalog protein quaternary and tertiary structural changes induced by the presence of H12.

PFG-NMR Self-diffusion Data: Shift to Monomer State at Specific Protein:H12 Ratios— To investigate how the size of PF4-M2 or Gro-α changed on binding H12, PFG-NMR self-diffusion measurements were performed at various protein (monomer):H12 ratios. For reference and calibration, Fig. 3*A* plots the temperature dependence of diffusion coefficients, D, for native PF4, IL-8 dimer, Gro-α dimer, and PF4-M2 in the absence of H12. The temperature dependence of D for PF4, PF4-M2, and IL-8 is linear with apparent activation energies of 4.7, 5, and 5 kcal/mol, respectively, and follows the activation energy expected for the self-diffusion of water, 4.8 kcal/mol. Thus, one can be confident that the aggregate state of these proteins remains essentially unchanged over this temperature range and that the distribution is homogeneous, *i.e.* multiple oligomerization states either are not present or are minimal. Therefore, it is reasonable to conclude that, as indicated in the literature, aggregation states for native PF4 (34) and IL-8 (35) are tetramer and dimer, respectively, at these concentrations. The temperature dependence of D for pure Gro-α at 10 mg/ml, although linear with an apparent activation energy value of 4.3 kcal/mol, does deviate more than expected for a single size species. Since Gro-α and IL-8 have nearly the same monomer molecular weight and are known to form the same type of dimers (20, 35), their dimers should display nearly the same diffusion coefficients. This is not the case with D values for Gro-α being larger than those for dimeric IL-8 and the difference in their apparent activation energies being 0.7 kcal/mol. Moreover, the temperature dependence for changes in aggregate state distributions for homologous α-chemokines PF4 (34) and NAP-2 (neutrophil activating peptide-2) (16) is small, suggesting a primarily entropy-driven process of self-association. This is consistent with the observed minimal change in activation energies for partially dissociated Gro-α. These diffusion data, therefore, indicate that Gro-α at this concentration is partly dissociated, more so at lower temperature as also observed with other α-chemokines. At 30 °C, a D value of about 15×10^{-7} cm^2/s is expected for compactly folded, monomeric Gro-α, assuming the ratio of monomer/dimer diffusion coefficients is similar to that of tetramer/dimer. This would indicate that, at 30 °C, this preparation of Gro-α is about 44% dimeric.

For PF4-M2, diffusion coefficients over the temperature range 10–40 °C are the same as those for IL-8, indicating that PF4-M2 is primarily dimeric under these solution conditions (6 mg/ml). This was unexpected since earlier studies (9) indicated that PF4-M2 at 6 mg/ml would be a mix of mostly dimers and tetramers. Moreover, ^{13}C and ^{15}N NMR relaxation data (T_1, T_2,

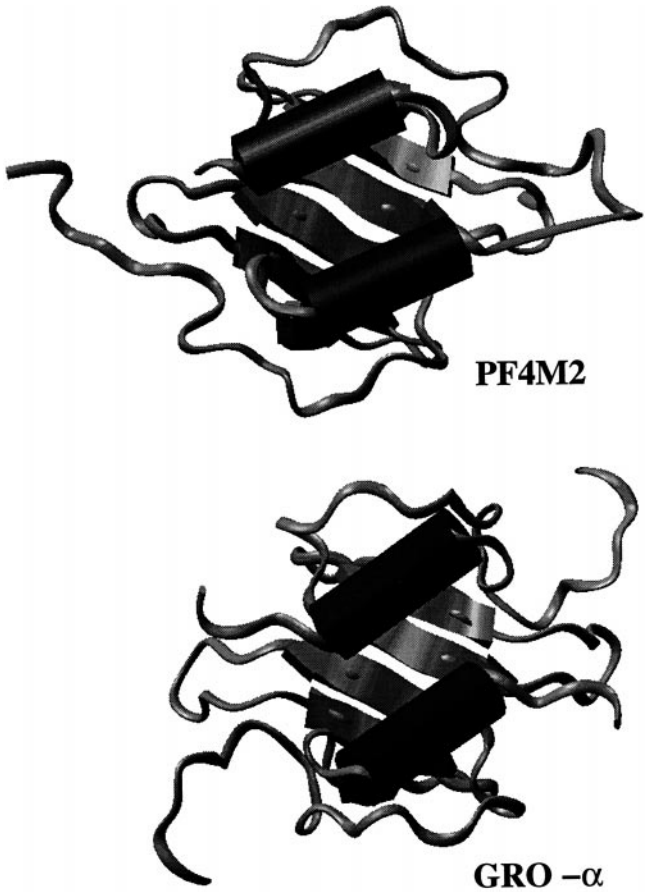

FIG. 2. **General fold of PF4-M2 and Gro-α AB-type dimers.** Both PF4 (PF4-M2) (9) and Gro-α (20) monomers exhibit similar three-stranded β-sheet with amphipathic C-terminal α-helix folded on to it. Shown are AB type dimers that are known to be formed by both PF4 (PF4-M2) and Gro-α. These dimers then associate to form asymmetric tetramers in PF4 or symmetric tetramers for PF4-M2.

and NOE)[2] yield rotational correlation times also consistent with PF4-M2 being primarily dimeric. These data contradict our earlier results regarding the aggregation states of PF4-M2 (9). Originally, the equilibrium between monomer, dimer, and tetramer states of native PF4 (34) and PF4-M2 (9) was interpreted via analysis of integrated intensities for three different Tyr-60 ring proton resonances, which arise from slow monomer-dimer-tetramer exchange on the chemical shift time scale. In the present $^{13}C/^{15}N$-enriched PF4-M2 preparation, only the Tyr-60 ring proton resonances corresponding to dimer and monomer (at lower concentration) states were observed. This is consistent with the present diffusion data on PF4-M2 and our earlier chemical cross-linking results (9), which indicated the presence of dimeric PF4-M2, but could not exclude the presence of tetramers. Furthermore, even though the PF4-M2 concentration used here (6 mg/ml) is not as high as that used in our previous study (18 mg/ml) on PF4-M2 (9), some PF4-M2 tetramer should have been present in solution. One explanation for this discrepancy is that the folding, and therefore the aggregate state distribution, of PF4 varies considerably from preparation to preparation (37). This may also occur with PF4-M2. In addition, the presence of PF4-M2 dimers and tetramers (9) was based on the identification of intersubunit NOEs. For AB-type dimers depicted in Fig. 2, intersubunit NOEs were numerous and unambiguous, clearly indicating that AB-type dimers were present in solution. AB-type dimers give a distinct pattern of NOEs between intersubunit anti-parallel β-strands (9, 20, 26). However, only a small set of intersubunit NOEs was identified between AB-type dimers, *i.e.* dimer-dimer association into tetramers. Reviewing those NOE data has indicated some ambiguities in the original inter-AB dimer (AC and AD) NOE assignments; this is currently being re-evaluated. For this H12 binding study, however, NOESY data on this preparation of PF4-M2 (data not shown) confirm the presence of AB-type (IL-8 or Gro-α like) dimers; previously identified tetramer NOEs (9) could not be observed. It is primarily because of this open question concerning variances from preparation to preparation in the aggregation state of PF4-M2 that the present study has included results on the interaction of H12 with homologous heparin-binding protein Gro-α, which is known to form only monomers and dimers in solution.

This preparation of PF4-M2 also still binds low molecular heparin (9,000-dalton cut-off) with a K_d of 5×10^{-8} M (9). Although H12 has a molecular mass of about 3,500 daltons, binding should still be relatively strong. In the present case, this binding constant was not measured due to limited amounts of H12. A titration with PF4-M2 and H12 was then performed. For this titration, aliquots of a concentrated solution of PF4-M2 were added to a solution of H12 to avoid precipitation of the complex since it had been observed previously that PF4 remained in solution only in the presence of excess heparin. An initial observation with PF4-M2 and H12 was that even titrating the protein into heparin produced some precipitation, which did become soluble after sitting at room temperature overnight. PF4-M2 diffusion data (35 °C) acquired at various PF4-M2:H12 molar ratios are plotted in Fig. 3*B*. Upfield methyl and methylene and downfield tyrosine PF4-M2 resonances were used to derive diffusion coefficients for the protein. H12 resonances generally overlapped with PF4-M2 resonances, *e.g.* αH, or were too close to the HDO resonance to be of value in deriving diffusion coefficients for H12 itself.

At a PF4-M2:H12 ratio of 2:1, *D* is significantly increased from that observed for pure PF4-M2, to a value expected for monomeric PF4-M2. Upon lowering the PF4-M2:H12 ratio from 2:1 to 1:6, *D* is decreased dramatically and appears to plateau off to a value that is less than that found for pure PF4-M2. Thus, when H12 is nearly equimolar with PF4-M2, protein dissociation occurs, whereas when it is in excess of the protein, the molecular size of PF4-M2 is increased. As will be evident later, NMR data indicate that the overall fold of PF4-M2 is highly perturbed at or near equimolar concentrations of H12, whereas the PF4-M2 conformation remains intact in the presence of excess H12. The smaller than expected *D* values at ratios of 1:3 and 1:6 could be attributed to a shift in the protein aggregate equilibrium, resulting in formation of some tetramer PF4-M2 and/or to complexation with H12. For tetrameric PF4-M2, *D* is expected to be about the same as that for native PF4, *i.e.* 10.1×10^{-7} cm^2/s (see Fig. 3*A*), and for this sample of pure PF4-M2, *D* is 13.2×10^{-7} cm^2/s, which is consistent with that expected for dimeric PF4. At ratios of 1:3 and 1:6, *D* values were, within error, essentially the same, *i.e.* $11.7 \times 10^{-7} \pm 0.6 \times 10^{-7}$ cm^2/s and $11.2 \times 10^{-7} \pm 0.3 \times 10^{-7}$ cm^2/s, respectively. This indicates that a limiting value has been reached. Since this *D* value falls short of that expected for tetramer PF4-M2 and little or no change in *D* is observed on going from a ratio of 1:3 to 1:6, it is more likely that the increase in molecular size is the result of H12 binding to PF4-M2. Using the Stokes-Einstein model, this *D* value corresponds to an apparent molecular mass of about 24,000 daltons. While this excludes formation of PF4-M2 tetramers (32,000 daltons), possibilities do include: 1) binding of about 4 molecules of H12

[2] V. Roongta, E. Ilyina, V. Daragan, and K. H. Mayo, unpublished results.

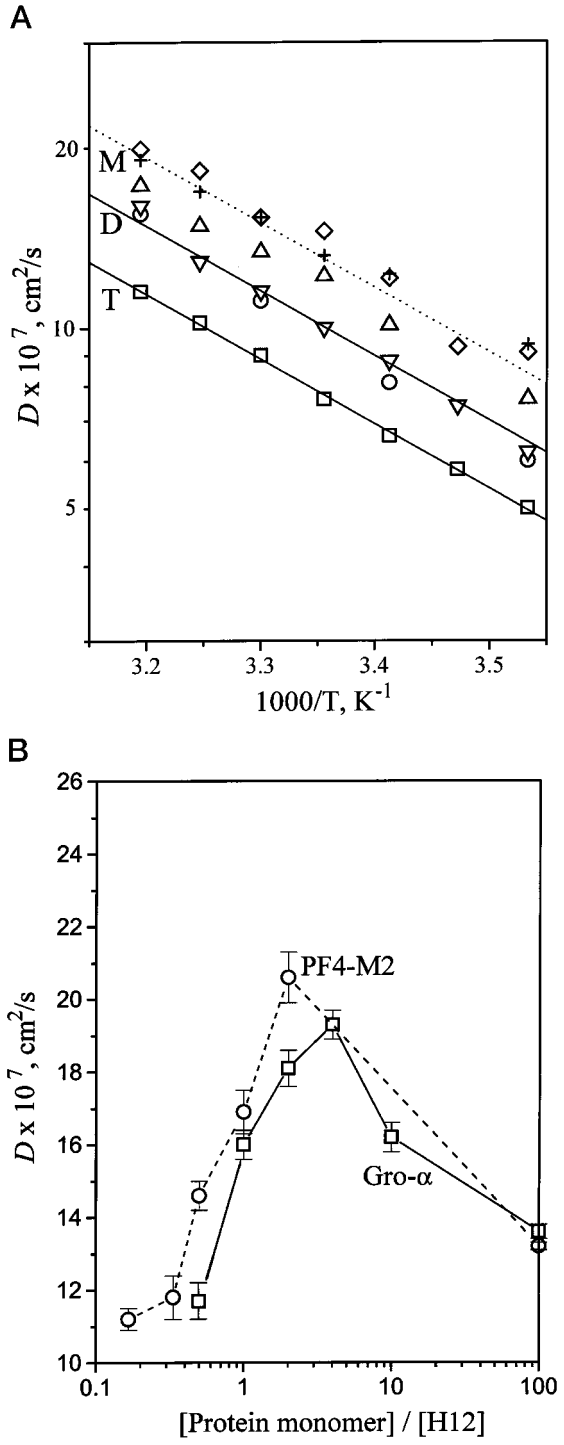

FIG. 3. **Translational diffusion coefficients.** *A*, the temperature dependence of translational diffusion coefficients is shown for native PF4 (30 mg/ml) (□), Gro-α (10 mg/ml) with (+, 1:1 molar ratio) and without (△) H12, IL-8 (10 mg/ml) (○), and PF4-M2 (6 mg/ml) with (◇, 1:1 molar ratio) and without (▽) H12. *Solid lines* indicate dimer (*D*) and tetramer (*T*) size, based on the diffusion of IL-8 and PF4, respectively. The *dotted line* is drawn for monomer (*M*) and is based on the D/T ratio being the same as the *M*/*D* ratio. *Solid* and *dotted lines* run parallel with the slope of the activation energy, E_a, for water. *B*, translational diffusion coefficients are plotted *versus* the protein:H12 molar ratio. Data were acquired at 30 °C and 35 °C for Gro-α and for PF4-M2, respectively. For pure protein, *D* values are indicated at the *right* of this plot for a high protein monomer:H12 molar ratio of 100:1. In both *A* and *B*, resonances from the upfield methyl and methylene and downfield tyrosine spectral region of the proteins were used to derive the diffusion coefficients.

(3,500 daltons each) to 1 molecule of PF4-M2 monomer, 2) binding of about 2 molecules of H12 to 1 molecule of PF4-M2 dimer, and 3) association of PF4-M2 into trimers. It is unlikely that trimers form because α-chemokines are not known to associate in this aggregate state; moreover, this would leave no room to account for some binding of H12 to the protein. Since chemical shifts of most resonances remain unperturbed by the presence of H12 at this protein:H12 ratio and intersubunit AB-type dimer NOEs are still observed, possibility 2 is the most probable.

Similar diffusion experiments were performed on the homologous α-chemokine Gro-α (30 °C) (Fig. 3*B*), which is known to self-associate only up to the dimer state. For Gro-α, the titration was performed in the opposite way from that with PF4-M2, in that H12 was now added to the protein; for the PF4-M2 titration, protein was added to a solution containing H12. Nevertheless, overall trends were observed to be the same. At less than equimolar concentrations of H12, *D* increased significantly for Gro-α as it did for PF4-M2. On changing the Gro-α (monomer):H12 ratio from 1:0 to 10:1 to 4:1, *D* reached its maximum value at 4:1, before decreasing from 2:1 to 1:1 to 1:2. At its peak (4:1), the value of *D* is consistent with Gro-α being in its monomeric state. At nearly this same ratio, H12 had the same effect on PF4-M2. Decreasing the Gro-α:H12 molar ratio from that point appears to reverse the H12-induced dissociation process and to shift Gro-α back toward its dimeric state. At least part of this decline in *D* values is probably the result of H12-Gro-α interactions. As was the case with PF4-M2 discussed above, the *D* value observed at the ratio of 1:2 (11.6×10^{-7} cm^2/s) is consistent with the binding of about 2 molecules of H12 to 1 molecule of dimeric Gro-α.

NMR and CD Data: Structural Transition in the Presence of H12—Since diffusion data indicate that, at certain protein:H12 ratios, H12 induces a shift in quaternary structure from dimer to monomer for both PF4-M2 and Gro-α, the question arose as to whether the tertiary structural fold was influenced by interaction with H12. To probe this question, ^{15}N/^{1}H HSQC two-dimensional NMR spectra were acquired at the same protein:H12 ratios (same samples) used for self-diffusion measurements. For pure PF4-M2, the HSQC contour plot (Fig. 4*A*) is the same as that obtained previously (9). At the PF4-M2:H12 ratio of 1:6, the HSQC appears mostly normal. However, by the ratio 1:2 (data not shown), it is evident that new ^{1}H/^{15}N cross-peaks are present in the mid-region of the spectrum. These are even more apparent at the ratio of 1:1 as shown in Fig. 4*B*. At this point, the HSQC spectrum appears highly perturbed. Most previously well resolved and dispersed ^{1}H resonances are weakened in intensity and are apparently broadened, while the new group of cross-peaks (7.8–8.6-ppm region in the ^{1}H dimension) have grown in intensity as the PF4-M2:H12 ratio increased. By a ratio of 2:1 (Fig. 4*C*), most native PF4-M2 cross-peaks have fallen into the noise, and the new group of cross-peaks, while still apparent, are also reduced in intensity and appear quite broad.

Since two sets of resonances (one for native PF4-M2 and one for the perturbed state) are apparent in HSQC spectra and one set grew in intensity as the other fell, this was a clear indication that the H12-induced shift in PF4-M2 structure occurs on the slow NMR chemical shift time scale. The apparent resonance broadening results from chemical exchange between the two states and/or from H12-induced conformational heterogeneity. In view of the diffusion data, this new set of resonances must be, in any event, associated with the lower aggregation (monomer) state of PF4-M2. Moreover, since the new set of resonances displays minimal ^{1}H chemical shift dispersion and is apparently clustered within the 7.8–8.6-ppm region, it is

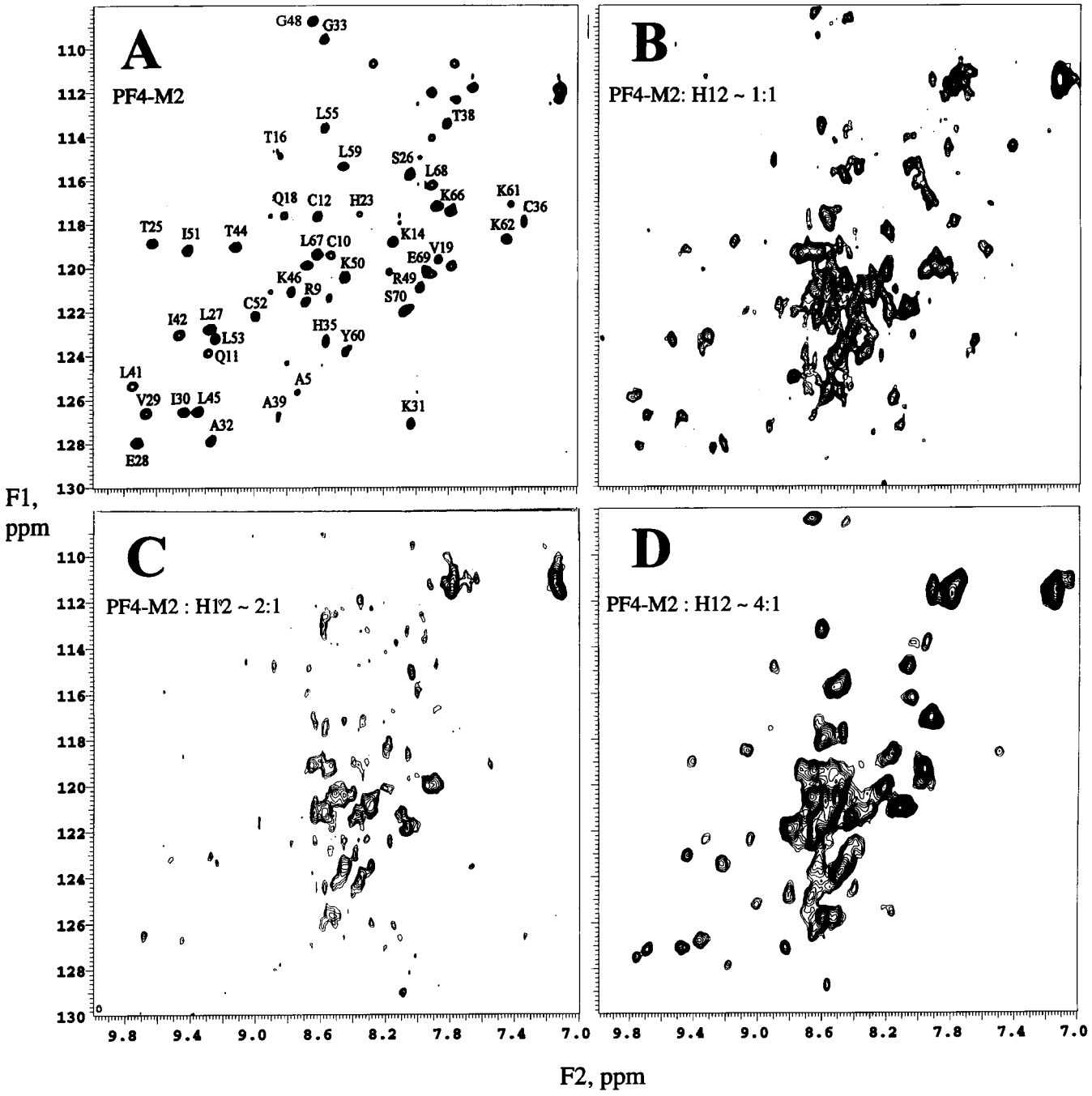

FIG. 4. **^{15}N HSQC spectra for PF4-M2 and for various PF4-M2:H12 molar ratios.** For pure PF4-M2, the HSQC spectrum in the *upper left panel* (*A*) is the same as that obtained previously (9). The other three panels show similarly acquired HSQC data obtained for various PF4-M2:H12 ratios of 1:1 (*B*), 2:1 (*C*), and 4:1 (*D*). These HSQC spectra were collected at 50 °C in the presence of 20 mM NaCl.

most probable that the H12-induced PF4-M2 monomer state is either considerably less folded than native PF4-M2 or considerably more conformationally flexible.

Having made these observations, the question of reversibility of this unfolding process arose. Since PF4-M2 in the new H12-induced state was isotopically labeled, this question was addressed by adding an equimolar amount of unlabeled PF4-M2 (not observed in ^{15}N/^{1}H HSQC spectra) to the sample already at the 2:1 PF4-M2(^{15}N-labeled):H12 ratio. As shown in Fig. 4*D* (ratio of 4:1), this appears to restore the native PF4-M2 ^{1}H resonance pattern, indicating that H12 binding to PF4-M2 is reversible. This in fact is similar to what was observed with Gro-α diffusion data, where at higher protein:H12 ratios, Gro-α appeared less structurally perturbed. It should also be noted that at this PF4-M2:H12 ratio of 4:1, resonances from both states remain quite broad, consistent with the presence of exchange on the slow-intermediate NMR chemical shift time scale of about 10–100 ms. Moreover, not all ^{1}H/^{15}N chemical shifts are exactly the same as for native PF4-M2. This indicates that, although the overall native fold has apparently returned, some perturbations to the native structure remain. These may be due to bound H12 in a now somewhat slightly modified PF4-M2 structure.

Similar HSQC spectral effects were observed for Gro-α in the presence of H12. Gro-α ^{15}N/^{1}H HSQC spectra collected at 30 °C for various Gro-α(monomer):H12 ratios are shown in Fig. 5*A*. Compared with the pure protein, addition of H12 induced the loss of ^{1}H chemical shift dispersion. Once again, a new set of

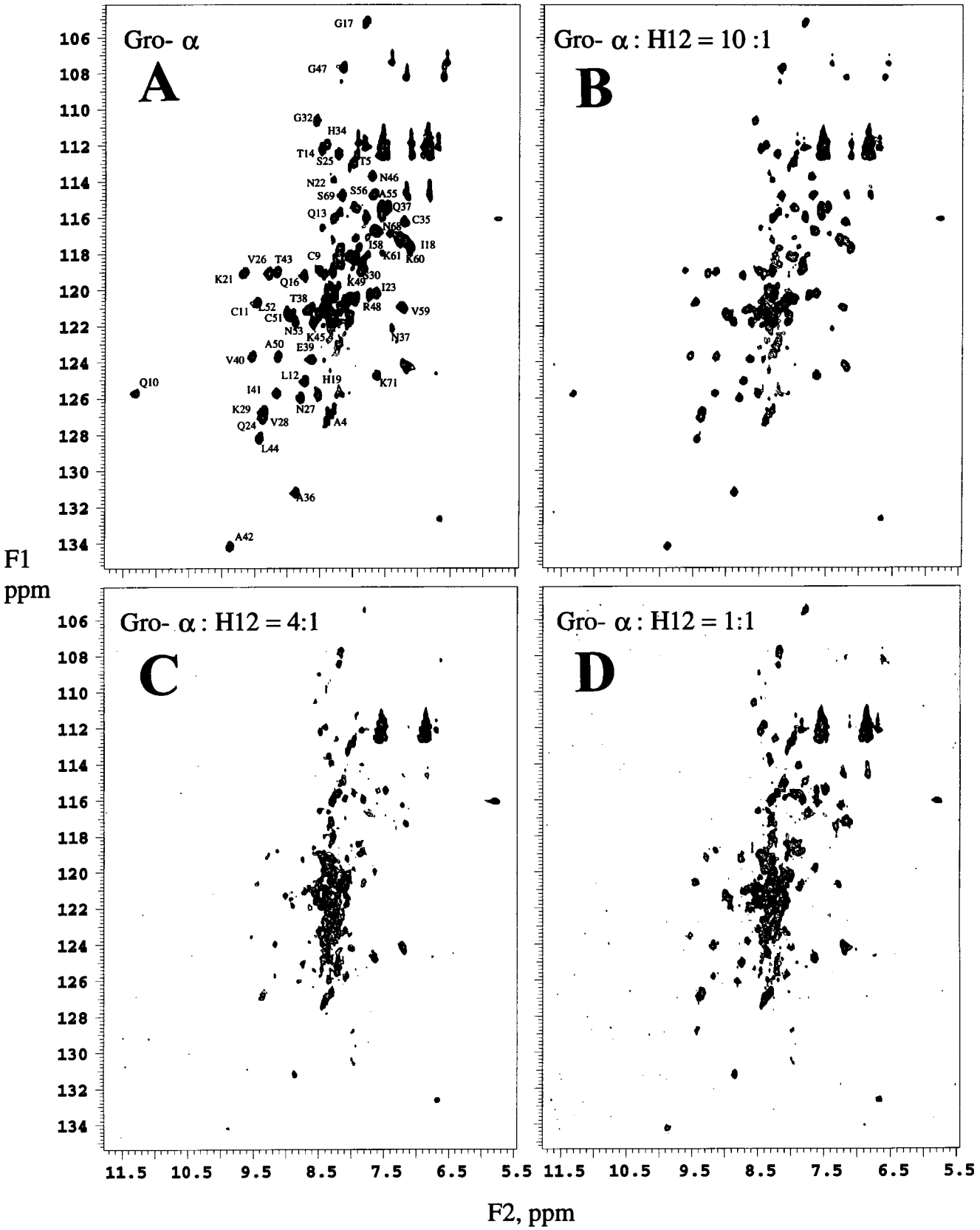

FIG. 5. **^{15}N HSQC spectra for Gro-α and for various Gro-α:H12 molar ratios.** The ^{15}N HSQC spectrum for pure Gro-α is shown in the *upper left panel* (*A*). The other three panels show similarly acquired HSQC data obtained for various Gro-α:H12 ratios of 10:1 (*B*), 4:1 (*C*), and 1:1 (*D*). These HSQC spectra were collected at 30 °C in the presence of 20 mM NaCl.

highly overlapping resonances appeared within the 7–8-ppm region and increased in intensity at the expense of native Gro-α resonances as the Gro-α:H12 ratio was changed from 10:1 (*B*) to 4:1 (*C*) or 2:1. As with PF4-M2, the native Gro-α and non-native Gro-α states are in slow exchange on the chemical shift time scale and minimal ^{1}H resonance dispersion (random coil shifts)

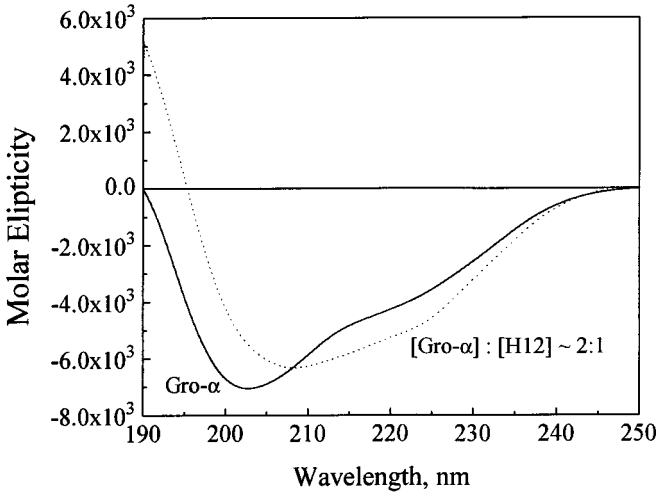

FIG. 6. **CD data for Gro-α (*solid line*) and for Gro-α in the presence of H12 (*dotted line*).** CD spectra were recorded at 30 °C in the presence of 10 mM potassium phosphate, pH 7, over a 190–250-nm range using a 0.5-mm path length, thermally jacketed quartz cuvette. The effective peptide bond concentration was about 2 mM. Spectra were signal-averaged eight times, and an equally signal-averaged solvent base line was subtracted.

in the non-native state suggests reduced structural integrity, *i.e.* increased flexibility and/or unfolding. At the 4:1 ratio, the HSQC spectrum indicates maximal change, although some greatly weakened, native Gro-α signals remain. Interestingly, the native-like ^{1}H chemical shift dispersion returns as the Gro-α:H12 ratio is further decreased (compare HSQC spectra acquired at ratios of 4:1 and 1:1 shown in Fig. 5, *C* and *D*). This trend agrees with that observed for PF4-M2. As the protein/heparin ratio is initially increased, structural integrity is reduced or lost; on further increasing this ratio, structural integrity returns. All $^{1}H/^{15}N$ resonances, however, do not return to their fully native chemical shift positions. Some remain chemically shifted. For PF4-M2, the signals, although regaining native-like dispersion, remain broader than those in the pure protein. Resulting resonance overlap precludes unambiguous assignments of resonances. For Gro-α, however, resonances do not appear to be broadened and remain relatively well resolved; some show very similar chemical shifts to resonances from pure Gro-α, while others are slightly chemically shifted. Those that are not shifted belong to residues located within the β-sheet domain and at the AB dimer interface. Residues that shift the most or do not appear in HSQC spectra are located within the loop containing residues His-19, Lys-21, and Ile-23 as well as residues Cys-9, Gln-10, Asn-46, and Ala-50, which are located in close proximity to this loop. The presence of heparin, therefore, must somehow still be affecting that region of the protein to which heparin interacts as noted earlier for PF4-M2. This will be discussed below for Gro-α at a lower Gro-α:H12 ratio.

Since for these NMR experiments, the concentration of PF4-M2 and Gro-α varied at different protein to H12 ratios, NMR spectra of control protein dilution experiments lacking H12 were run. For the protein concentrations under investigation, no differences in chemical shift patterns were observed.

Since NMR data indicate that, at the appropriate protein:H12 ratio, H12 induces a conformational transition in the protein to what might be random coil, and at the very least, non-native, CD data were acquired to establish if secondary structure were also lost. CD traces for Gro-α in the absence and presence of H12 (protein:H12 ratio of 2:1) are shown in Fig. 6. In the absence of H12, deconvolution of the CD trace (33) yields percent structure content of 15% helix, 29% β-sheet, 26% turn, and 30% other. This distribution is expected from the known structure of Gro-α (20). At a Gro-α:H12 ratio of 2:1 where the shift to monomer has already occurred, the 220-nm band is stronger, indicating a conformational shift to more α-helix. Deconvolution of this CD trace yields a structural composition of 20% helix, 29% β-sheet, 25% turn, and 26% other. This 5% increase in helix content is consistent with the addition of 3–4 residues to those helix residues normally found in Gro-α. Since helix conformation in Gro-α (and in all α-chemokines) is primarily located within the C-terminal segment, it is tempting to suggest that this stretch of helix may be extended by one turn on interacting with H12. Alternatively, some other segment, possibly the short helical loop at residues 20–24, may be helically extended. In any event, this conformational transition is linked to H12-induced subunit dissociation. Similar results were observed with PF4-M2.

H12 Binding to Native PF4-M2 at Low PF4-M2:H12 Ratio—H12 binding to PF4-M2 and to Gro-α at low protein:H12 ratios, is supported by three observations: 1) diffusion coefficients are reduced relative to those for the dimeric species, 2) resonance line widths are increased, and 3) spin-lattice (T_1) relaxation rates (data not shown) are decreased. While for PF4-M2 these changes could potentially be associated with self-association to the tetramer state as opposed to H12 binding, this would not be the case for Gro-α. Gro-α forms only monomers and dimers in solution, and the diffusion coefficient for Gro-α:H12 at a ratio of 1:2 indicates the presence of an apparent molecular weight larger than that expected for dimeric Gro-α. Only H12 binding to Gro-α could account for this. Moreover, for PF4-M2, titration with H12 at ratios of 1:3 and 1:6 showed a limiting *D* value, indicating a molecular species much smaller than that expected for tetramer PF4; this therefore is most likely explained by H12 binding to PF4-M2 as discussed above. While changes in protein aggregation state and overall folding and/or conformational flexibility indeed occur during the protein:H12 titration, H12 binding to protein at low protein:H12 ratios is the most likely scenario.

At a PF4-M2:H12 ratio of 1:3 where resonance dispersion as observed in native PF4-M2 is still apparent, three-dimensional NMR HCCH-TOCSY data were collected to assess if side-chain chemical shifts had been perturbed. This information may be used to argue for H12 interaction at a particular site. Three HCCH ^{13}C planes are shown in Fig. 7 for native PF4-M2 (*left panels A*, *C*, and *E*) compared with PF4-M2 in the presence of a 3-fold molar excess of H12 (*right panels B*, *D*, and *F*).

Resonances for some key heparin binding residues, among others, have been labeled in Fig. 7 in the panels for native PF4-M2. Note that, in the presence of H12 (*panels B*, *D*, and *F*), many cross-peaks are not observed, and those that remain display essentially the same chemical shifts as in native PF4-M2. This is consistent with HSQC data discussed previously and supports the proposal that the overall structure for most of the PF4-M2 population is conserved at this particular protein:H12 ratio. It is, however, those resonances which no longer appear in the spectrum that are intriguing. For the resonances labeled in Fig. 7, those for Ala-32, Ala-39, Ala-57, Arg-9, Arg-49, and most of the lysine resonances are still apparent in the presence of H12. Others, like Arg-20 and Arg-22, however, are no longer apparent. By mapping all resonances that are no longer readily observed, onto the structure for PF4-M2 (9), it is evident in the AB dimer shown as a space-filling model in Fig. 8 (structure at the *right*) that most are localized to one region (*darker shadings*) around the Arg-20-His-23 loop and including Lys-46 and Asn-47. This region has already been identified as a primary site for interaction with heparin (9). The binding site shown is on the B-subunit; the same site on the A-subunit is partially visible at the extreme far right of the AB dimer.

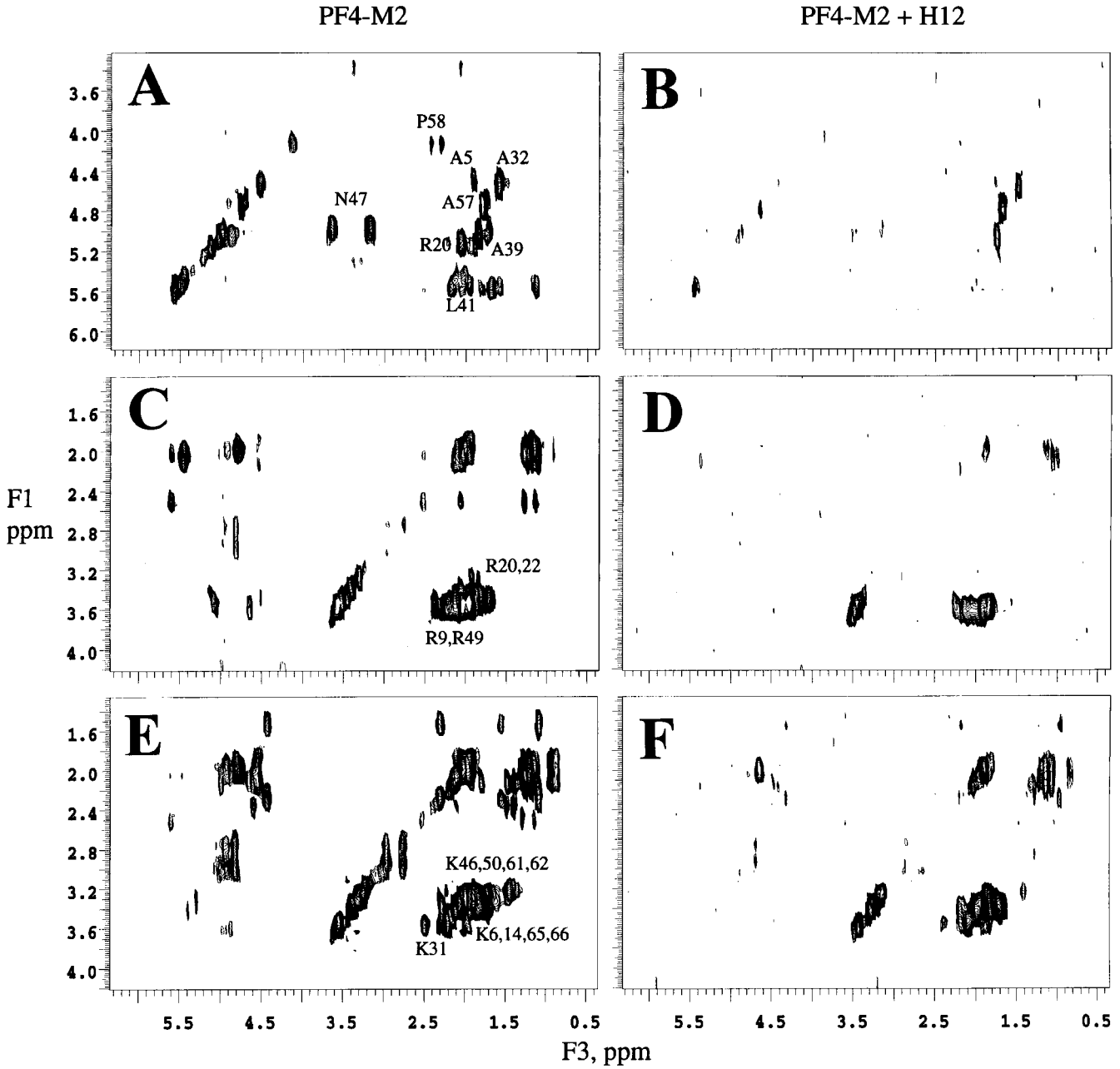

FIG. 7. **HCCH-TOCSY data for PF4-M2 and for PF4-M2 with 3-fold excess of H12.** Shown are three ^{13}C two-dimensional planes at 55.7, 46.4, and 45.2 ppm, from top to bottom, respectively, in the absence (*A*, *C*, and *E*) and presence (*B*, *D*, and *F*) of H12. In the presence of H12, many cross-peaks are not observed, and those that remain display essentially the same chemical shifts as native PF4-M2. These three-dimensional NMR data sets were collected at 50 °C in the presence of 20 mM NaCl.

Interestingly, resonances from C-terminal lysines, which also form part of the proposed heparin binding domain (11–13), are little affected. As oriented in Fig. 8, the C-terminal helix runs along the top of the AB dimer structure. A tetramer of PF4-M2 (almost the same tetrameric structure for native PF4) is shown at *left* to indicate the assembly of A, B, C, and D subunits as well as the proximity of this affected region between BC subunits.

All carbon and proton planes were examined for the possibility that cross-peaks may shift from one plane into another. This is not the case. Resonances that are not observed in a given plane with pure PF4-M2 are indeed absent from all planes. The disappearance of some resonances while others remain was surprising. Two explanations come to mind. 1) H12 interacts tightly at this site, but binding is heterogeneous, which results in formation of multiple binding states and, therefore, multiple resonances for these residues thereby lowering their signal into the noise level; or 2) H12 interacts at this site and does so in an equilibrium with free H12 that occurs on an intermediate chemical shift time scale (relatively weaker binding) such that resonances associated with these residues are highly broadened and therefore not observed. The first scenario is more likely since the number of H12 molecules exceeds that of the protein, and most of the protein should be in the H12-bound state. In any event, one conclusion that may be drawn is that H12 interacts primarily with this site on PF4-M2. Moreover, H12 interactions at this site on the protein probably induce the observed conformational transition in PF4-M2. The excess of H12 appears to prevent the denaturation of the protein as observed at higher protein:H12 molar ratios.

Since ^{13}C-enriched Gro-α was not available, similar HCCH-TOCSY experiments could not be performed. However, on re-

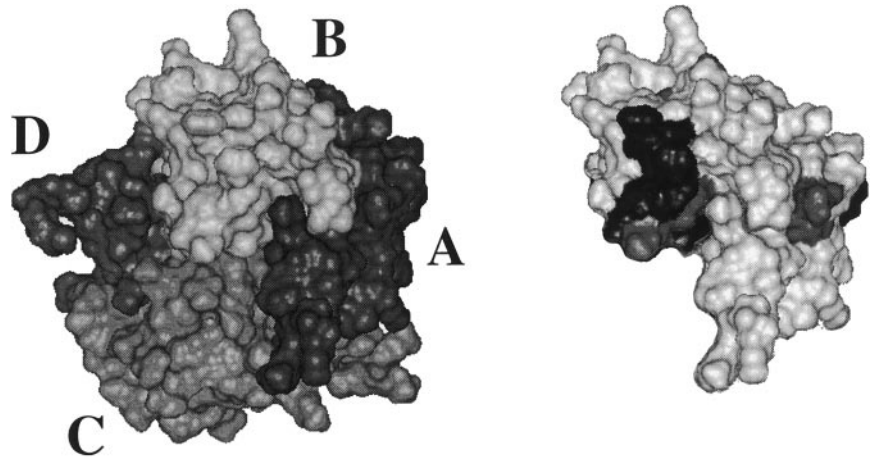

FIG. 8. **PF4-M2 residues most affected by H12 binding.** A space-filling model of the PF4-M2 tetramer (subunits labeled *A–D*) is shown at the *left* to indicate positioning of the four subunits, and at the *right*, the AB dimer of PF4-M2 is shown highlighting those residues whose resonances are most affected (*darker shading*) by the presence of H12 in 3-fold molar excess of PF4-M2 as discussed in the text.

viewing HSQC data for Gro-α, it is apparent that resonances associated with residues around the same loop region as in PF4-M2 do demonstrate the largest chemical shift changes in the presence of H12. This suggests that H12 is binding at or near the same site in Gro-α and presents a commonality in the interaction of H12 with at least these two α-chemokines.

Effects to H12 upon Interaction with PF4 and Gro-α—During collection of H12 titration data with PF4-M2 and Gro-α, ^{1}H TOCSY spectra were acquired to observe effects on H12 proton resonances. In the presence of protein, H12 resonances, little perturbed at low protein:H12 molar ratios, became somewhat shifted and increasingly broadened as the protein:H12 ratio was increased. Above a ratio of 1:1, H12 resonances significantly decreased in intensity and were less obvious, most likely due to exchange broadening. ^{1}H TOCSY spectra showing H12 ^{1}H cross-peaks are exemplified in Fig. 9 for Gro-α:H12 ratios of 1:1 (*panel A*), 2:1 (*panel B*), and 4:1 (*panel C*). These ratios correspond to the increasingly altered conformational state of the protein discussed above. At the ratio 1:1 (*panel A*), H12 resonances have nearly the same chemical shifts as free H12. Maximal chemical shift changes are less than 0.1 ppm for anomeric proton resonances, which are particularly sensitive to ring conformation and ring orientations about glycosidic linkages. When the protein:H12 ratio is increased to 2:1 and then to 4:1, most H12 cross-peaks can not be observed (*panels B* and *C*). One exception is for resonances associated with the nonreducing terminal iduronate residue whose resonances appear to be unaffected by the presence of protein. This is probably the result of that residue being highly mobile and/or not interacting with the protein. Compare these data to those HSQC data on Gro-α (Fig. 5, *C* and *D*) at the same 4:1 and 1:1 ratios. Notice that, at 4:1, most protein cross-peaks characteristic of well folded regions display highly diminished intensities or are absent, while cross-peaks within the mid-region of the spectrum are relatively most intense. These mid-region cross-peaks are also evident at the 10:1 ratio (Fig. 5*B*). As discussed previously, it appears that these populations, *i.e.* Gro-α:H12 bound and free, are in slow exchange on the chemical shift time scale. As the ratio goes to and then below 1:1, native Gro-α cross-peaks return.

It is interesting to note that in the presence of PF4-M2, H12 iduronate resonances are slightly more shifted than glucosamine resonances, whereas, in the presence of Gro-α, H12 glucosamine resonances are more shifted, suggesting that different H12 sugar residues, iduronates *versus* glucosamines, may mediate interactions with PF4-M2 and Gro-α, respectively. As discussed above, however, the primary site of interaction on either protein does appear to be the same. Even though PF4-M2 and Gro-α are both cationic proteins, the presentation of charged groups and other residues on their surfaces is different and may explain this observation. Compared with PF4-M2, for example, Gro-α has one acidic glutamate instead of a basic lysine residue within the C-terminal helix region, as well as . . . HPKN . . . rather than . . . RPRH . . . within the N-terminal helical loop region.

As the protein:H12 ratio is decreased further below 1:1, H12 resonances become more prominent and narrower, and their chemical shift positions eventually become the same as those observed for free H12. This is to be expected when H12 is in excess. However, it was anticipated that perhaps a second population of H12 resonances resulting from slow H12-protein exchange might have been observed. This was not the case. This observation is related to that made in the HCCH-TOCSY data with PF4-M2 in the presence of a 3-fold molar excess of H12, where a number of protein cross-peaks were not observed (Fig. 7). As proposed earlier, either H12-protein binding is tight and heterogeneous or H12-protein exchange occurs on an intermediate chemical shift time scale.

DISCUSSION

In the presence of excess heparin dodecasaccharide, binding to these native α-chemokine proteins occurs primarily at the N-terminal helical loop region (residues 20–23 in PF4), which leads into the first β-strand. At limiting concentrations of H12, however, PF4-M2 and Gro-α quaternary and tertiary structures are disrupted. One explanatory scenario, which can be broken down in three main steps, is sketched out in Fig. 10. The *first step* is that in the presence of excess heparin oligosaccharide, α-chemokine dimers bind H12. The excess of heparin oligosaccharide may in fact stabilize the protein against denaturation observed to occur at higher protein:H12 ratios. This would explain why at PF4-M2(monomer):H12 ratios of 1:6 and 1:3, diffusion coefficients measured using protein resonances decreased indicating formation of a species with a larger radius, *i.e.* H12 is bound to PF4-M2. In the *second step* as the protein concentration is increased further, protein molecules are in excess and H12 binding to only one subunit of an aggregate may disrupt the domain interface via conformation changes to perturb or disturb the interface resulting in dissociation and partial unfolding and/or increased flexibility of the fold. The protein maintains a similar secondary structural distribution as the native species, but with increased helix content. This step establishes a possibly new mode of heparin-protein interaction. These structural perturbations are maximal at protein (monomer):H12 ratios of 2:1 to 4:1, but are most certainly present to some degree at higher ratios. The binding constant for heparin (H12) to this partially folded state

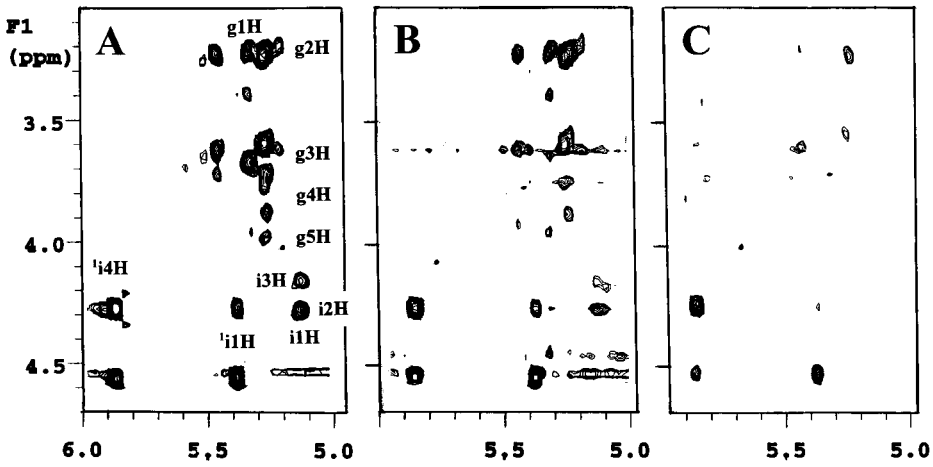

FIG. 9. **^{1}H TOCSY data for H12 anomeric ^{1}H region in the presence of Gro-α.** TOCSY data are plotted for the anomeric ^{1}H region of H12 in the presence of Gro-α for Gro-α:H12 ratios of 1:1 (*A*), 2:1 (*B*), and 4:1 (*C*). Individual resonances for internal disaccharide repeating units could not be resolved. *Lowercase letters g* and *i* refer to glucosamine and iduronate residues, respectively. *Numbers* and *uppercase letters*, *e.g. 1H* or *2H*, refer to a proton within either of these two sugar rings. Only the non-reducing end sugar ring could be unambiguously assigned; it has been labeled with a *superscript number* at the *left*.

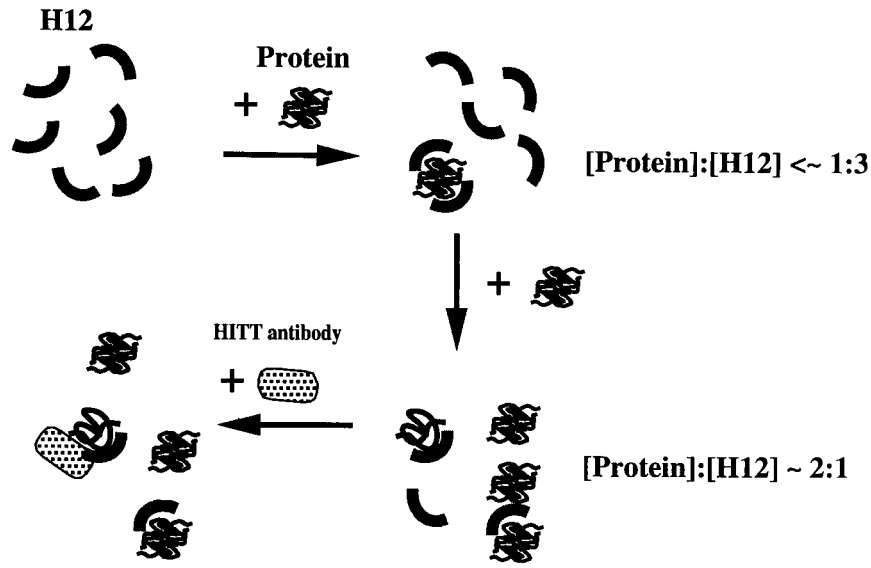

FIG. 10. **Scenario for the binding of heparin oligosaccharide H12 to α-chemokine dimers, induction of a partially folded protein state, and binding of HITT antibody to the heparin-induced partially folded state.** In the *upper left*, free H12 in solution is shown. Protein (PF4 or Gro-α) in the presence of an excess of H12 forms a protein-H12 complex (*upper right*). Addition of more protein induces a conformational change in the protein leading to partial unfolding (*lower right*) as discussed in the text. HITT antibody recognizes and binds to the partially folded (but not the folded) state of PF4 (*lower left*). The specific epitope is unknown.

is unknown, but is probably less than that for the native protein.

Addition of more protein to raise the protein:H12 ratio even further leads to the *third step*: conformational transition back to a more native-like fold. This conclusion is based on the observation of a similar dispersion of ^{1}H/^{15}N resonances in the newly folded state compared with that of the native protein. Since some ^{1}H/^{15}N resonances in this state are slightly chemically shifted from their positions in the native state, minor structural perturbations are apparent; nonetheless, the overall tertiary fold is regained. These resonance shifts and broadening are probably the result of heparin binding to the protein and/or some process of heparin-protein chemical exchange. Regaining of a native-like resonance pattern at higher protein:H12 ratios supports the idea that H12-induced unfolding is stoichiometrically limiting, *i.e.* a certain number of protein molecules can interact with one H12 thereby inducing the unfolding transition. The binding of more than one protein molecule to a molecule of a heparin oligosaccharide is not unique and has been observed previously. DiGabriele *et al.* (38) reported that dimers of FGF-1 exist with their monomers being bridged exclusively by a heparin decasaccharide, *i.e.* no protein-protein interactions are observed. Protein binding to the heparin decasaccharide occurs at opposite sides of the heparin helix. In the case of FGF-1, heparin-induced unfolding, however, apparently does not occur as it does with α-chemokines.

The primary site at which H12 binds to PF4-M2 (. . . RPRH . . . loop) resides within a path of positively charged residues that runs perpendicular to the C-terminal α-helix, and is in a region on the protein surface opposite to the AB dimer anti-parallel β-sheet interface (12, 13). One might ask how realistic this binding mode is, given the fact that only a dodecasaccharide fragment of heparin was used in this study. In a computational modeling study of heparin binding to native PF4, Stuckey *et al.* (12) concluded that a hexadecasaccharide or an octadecasaccharide heparin fragment would provide the minimal length to fully wrap around AB type PF4 dimers. On the other hand, in an experimental NMR study (13), it was observed that low molecular mass, heterogeneous heparin (9,000-dalton cut-off) interacts with residues within this same path of positively charged groups and perhaps more importantly that Arg-20 and Arg-22 were crucial to this binding process, even more crucial than the four C-terminal lysines proposed earlier as being the primary mediators of heparin binding to PF4 (10, 11). Furthermore, these HCCH-TOCSY NMR data on PF4-M2:H12 were acquired at about the same ratio used in that NMR study (13). Taken together, this information supports the idea that use of heparin dodecasaccharide does provide a reasonable model to probe the actual binding of heparin to PF4. Interestingly, this loop region (residues 20–24)

also appears to be the region where H12 preferentially interacts with the homologous α-chemokine Gro-α.

The observation that H12 interacts preferentially with residues within this Arg-20/Arg-22 loop region rather than with lysines from the C-terminal α-helix, is supported by previous findings that sulfated GAGs interact more strongly with arginines than they do with lysines. By examining the frequency of amino acids in proteins at sites known to bind heparin as well as combinatorial peptides with high affinity for heparin and heparan sulfate agarose, a preference for arginine over lysine, with histidine falling a distant third in modulating GAG binding, was observed (39). Gelman *et al.* (40) demonstrated that a polyarginine α-helix denatured at a higher temperature when bound to GAGs than did an analogous polylysine polymer. Arginines are also essential for the binding of thrombin and antithrombin-III to heparin (41, 42). Other studies in model polypeptides showed also that arginines bind more tightly to heparin than do lysines (43–45). Recently, from x-ray crystal studies of bFGF co-crystallized with heparin derived tetra- and hexasaccharides (46), it was found that Arg-121 of bFGF forms a high affinity binding site that interacts with acidic groups on the heparin hexasaccharide, whereas a lower affinity site was formed with lysines.

Although the primary H12 binding site on PF4-M2 and Gro-α appears to be the same (N-terminal helical loop leading into the first strand of the β-sheet), binding is mediate via different residues on each protein. This would certainly contribute to differences in the strength of heparin binding to each protein. In addition, the binding site on H12 appears to be different for each α-chemokine. For PF4-M2 binding, iduronate residues on H12 appear to provide the primary interaction sites, whereas for Gro-α, glucosamines appear to be the primary mediators of binding. These observations are not so unusual. Within the FGF protein family, for example, no residue within the heparin binding region is completely conserved, and even though electrostatic interactions are known to be crucial for binding, even the charge of the residue side chain fails to be strictly maintained (47). In this respect, different members of the FGF family also utilize different contacts for binding to heparin. In terms of the binding sites on heparin oligosaccharides, FGF-2 requires the 2-*O*-sulfate but not the 6-*O*-sulfate, whereas FGF-1 requires both and FGF-4 can bind heparin in the absence of either 2-*O*- or 6-*O*-sulfate (48, 49). Furthermore, FGF-2 makes a specific contact to the 2-*O*-sulfate of iduronate through the Gln-135 side chain (46), such that substitution of this residue by methionine in FGF-4 would prevent this interaction, consistent with the observation that FGF-4 can bind heparin in the absence of 2-*O*-sulfate groups (48). Moreover, FGF-1 utilizes one binding site to interact with heparin in two different orientations, *i.e.* with different groups from heparin. Given these observations, it appears that, while the heparin binding site within a given protein family is conserved, the character of the residues mediating binding are different and heparin interacts with that site(s) by adjusting/selecting which of its saccharide residues and/or groups best mediate the interaction.

In the second step of our model, the H12-induced protein conformational transition to a partially folded state is quite novel in the way of thinking about how heparin affects and binds to a protein. However, it does help to explain, on a molecular level, the immune disorder heparin-induced thrombocytopenia/thrombosis (HITT). In a clinical setting, some patients treated with heparin develop the pathology of thrombocytopenia and a subset of these patients experience arterial or venous thromboembolism. These complications, which occur in the presence of pharmacologic concentrations of heparin, are caused by an unusual type of antibody, specific for complexes formed between heparin and PF4 (50). Antibody complexes (PF4/heparin/antibody), formed on or in close proximity to the platelet membrane, interact with platelet Fc receptors to induce platelet activation and are thus important in the pathogenesis of HITT. The epitope(s) on PF4-heparin complexes recognized by these HITT antibodies have not been identified, and it is uncertain whether a preferred site on the PF4-heparin complex is targeted (51). What relates this phenomenon to observations made in the present biophysical study is that only certain PF4:heparin ratios are highly effective at binding HITT antibody (52). The most effective PF4(monomer):heparin ratio appears to be between about 8:1 and 4:1, although other results show similar increase of HITT antibody binding when PF4 and heparin are present at equimolar concentrations (53).

These current biophysical studies indicate that at a ratio of about 2:1 to 4:1, structural perturbations to PF4-M2 are maximal and shift the native fold into a partially folded, perhaps molten globule-like, state. The biophysically derived protein: heparin ratio falls directly within the range of values observed for maximal HITT antibody binding to PF4. Assuming that these biophysical studies can be extended into the realm of cell biology, it is probable that the HITT antibody actually recognizes the partially folded species of PF4 as depicted in Fig. 10. This may explain why only certain antibodies specific for PF4: heparin are associated with adverse symptomatology (54). Furthermore, even though heparin is usually found to stabilize the conformation of a protein against thermal (55, 56) or chemical denaturation (57), it can function in various ways. For example, the addition of heparin tetra- and decasaccharides to a solution of aFGF induces formation of higher molecular weight aggregates (58). Here, at certain protein:H12 ratios, H12 is observed to induce a conformational transition to a partially folded state in both PF4-M2 and Gro-α. This is not the first observation that heparin binding is related to a denatured protein state. Vitronectin binding to a heparin column was enhanced when the protein was denatured either chemically (urea or acid) or thermally (59). Heparin has also been shown to cause a rapid, time- and temperature-dependent conformational alteration of trypsin leading to irreversible denaturation and degradation of the protein (36). Interestingly, the most significant conformational alterations to trypsin were observed to occur at a nearly equimolar proteinase-to-heparin ratio, similar to that observed in the present study.

A general hypothesis that arises from the present study is that some proteins, which bind to heparin, or to heparan sulfate found on the surface of all eukaryotic cells, could be induced to shift conformation on binding the GAG. The role of GAGs on the surface of cells is yet mostly unknown. The effect observed here is that at certain ratios of protein:H12, the protein undergoes a conformational transition to a less folded state, which probably makes it more susceptible to antibody binding and perhaps proteolysis *in situ*. *In vivo*, this would depend on the affinity of a given protein for polysulfated GAGs presented on the cell surface. Weak binding would leave little bound to these GAGs, and strong binding, as with PF4, would have a significant population bound, *e.g.* if a particular protein were expressed at too high a level, some would be bound to cell surface heparan sulfate and may become partially unfolded. This shift in folding could promote clearance via antibody binding or general proteolysis. The HITT antibody discussed above may in fact be specific for partially folded proteins and function as a clearance mechanism for non-native species.

REFERENCES

1. Jeanloz, R. W. (1975) *Adv. Exp. Med. Biol.* **52,** 3–12
2. Tyrrell, D. J., Ishihara, M., Rao, N., Horne, A., Kiefer, M. C., Stauber, G. B., Lam, L. H. & Stack, R. J. (1993) *J. Biol. Chem.* **268,** 4684–4689

3. Lyon, M., Deakin, J. A., Mizuno, K., Nakamura, T. & Gallagher, J. T. (1994) *J. Biol. Chem.* **269,** 11216–11223
4. von Boeckel, C. A. A., Grootenhuis, P. D. J. & Visser, A. (1994) *Struct. Biol.* **1,** 423–425
5. Mire-Slius, A. & Thorpe, R. (eds) (1998) *Cytokines*, Academic Press, San Diego
6. Witt, D. P. & Lander, A. D. (1994) *Curr. Biol.* **4,** 394–400
7. Davie, E. W., Fujikawa, K. & Kisiel, W. (1991) *Biochemistry* **30,** 10363–10370
8. Zhang, X., Chen, L., Bancroft, D. P., Lai, C., K., & Maione, T. E. (1994) *Biochemistry* **33,** 8361–8366
9. Mayo, K. H., Roongta, V., Ilyina, E., Millius, R., Baker, S., Quinlan, C., La Rosa, G. & Daly, T. J. (1995) *Biochemistry* **34,** 11399–11409
10. Loscalzo, J., Melnick, B. & Handin, R. I. (1985) *Arch. Biochem. Biophys.* **240,** 446–455
11. Cowan, S. W., Bakshi, E. N., Machin, K. J. & Isaacs, N. W. (1986) *Biochem. J.* **234,** 485–488
12. Stuckey, J. A., St. Charles, R. & Edwards, B. F. P. (1992) *Proteins Struct. Funct. Genet.* **14,** 277–287
13. Mayo, K. H., Roongta, V., Ilyina, E., Dundas, M., Joseph, J., Lai, C. K., Maione, T. & Daly, T. J. (1995) *Biochem. J.* **312,** 357–365
14. Pervin, A., Gallo, C., Jandik, K., Han, X.-J. & Linhardt, R. J. (1995) *Glycobiology* **5,** 83–95
15. Linhardt, R. J., Rice, K. G., Kim, Y. S., Lohse, D. L., Wang, H. M. & Loganathan, D. (1988) *Biochem. J.* **254,** 781–787
16. Yang, Y., Mayo, K. H., Daly, T. J., Barry, J. K. & La Rosa, G. L. (1994) *J. Biol. Chem.* **269,** 20110–20118
17. Smith, P. K., Krohn, R. I., Hermanson, G. T., Mallia, A. K., Gartner, F. H., Provenzano, M. D., Fujimoto, E. K., Goeke, N. M., Olson, B. J. & Klenk, D. C. (1985) *Anal. Biochem.* **150,** 76–85
18. Lowry, O. H., Rosebrough, N. J., Farr, A. L. & Randall, R. J. (1951) *J. Biol. Chem.* **193,** 265–270
19. Waddell, W. J. (1956) *J. Lab. Clin. Med.* **48,** 311–314
20. Fairbrother, W. J., Reilly, D., Colby, T., Hesselgesser, J. & Horuk, R. (1994) *J. Mol. Biol.* **242,** 252–270
21. Bax, A. & Davis, D. G. (1985) *J. Magn. Reson.* **65,** 355–360
22. Jeener, J., Meier, B., Backman, P. & Ernst, R. R. (1979) *J. Chem. Phys.* **71,** 4546–4550
23. Wider, G., Macura, S., Anil-Kumar, Ernst, R. R. & Wüthrich, K. (1984) *J. Magn. Reson.* **56,** 207–234
24. Grzesiek, S. & Bax, A. (1993) *J. Am. Chem. Soc.* **115,** 12593–12594
25. Kay, L. E., Keifer, P. & Saarinen, S. (1992) *J. Am. Chem. Soc.* **114,** 10663–10668
26. Clore, G. M., Bax, A., Driscoll, P. C., Wingfield, P. T. & Gronenborn, A. M. (1990) *Biochemistry* **29,** 8172–8184
27. Zhang, O., Kay, L. E., Olivier, J. P. & Forman-Kay, J. D. (1994) *J. Biomol. NMR* **4,** 845–858
28. Wijmenga, S. S., van Mierlo, C. P. M. & Steensma, E. (1996) *J. Biomol. NMR* **8,** 319–330
29. Ilyina, E., Roongta, V., Pan, H., Woodward, C. & Mayo, K. H. (1997) *Biochemistry* **36,** 3383- 3388
30. Altieri AS, Kinton DP & Byrd RA. (1995) *J. Am. Chem. Soc.* **117,** 7566–7567
31. Gibbs, S. J. & Johnson, C. S. (1991) *J. Magn. Reson.* **93,** 395–402
32. Cantor, C. R. & Schimmel, P. R. (1980) *Biophysical Chemistry*, W. H. Freeman & Co., New York
33. Sreerama, N. & Woody, R. W. (1993) *Anal. Biochem.* **209,** 32
34. Mayo, K. H. & Chen, M. J. (1989) *Biochemistry* **28,** 9469–9478
35. Clore, G. M., Appella, E., Yamada, M., Matsushima, K. & Gronenborn, A. M. (1989) *J. Biol. Chem.* **264,** 18907–18911
36. Finotti, P. & Manente, S. (1994) *Biochim. Biophys. Acta* **1207,** 80–87
37. Barker, S. & Mayo, K. H. (1995) *FEBS Lett.* **357,** 301–304
38. DiGabriele, A. D., Lax, I., Chen, D. I., Svahn, C. M., Jaye, M., Schlessinger, J. & Hendrickson, W. A. (1998) *Nature* **393,** 812–817
39. Caldwell, E. E. O., Nadkarni, V. D., Fromm, J. R., Linhardt, R. J. & Weiler, J. M. (1996) *Int. J. Biochem. Cell Biol.* **28,** 203–216
40. Gelman, R. A. & Blackwell, J. (1974) *Biopolymers* **13,** 139–156
41. Pomerantz, M. W. & Owen, W. G. (1978) *Biochim. Biophys. Acta* **535,** 66–77
42. Machovich, R., Staub, M. & Patthy, L. (1978) *Eur. J. Biochem.* **83,** 473–477
43. Mikhailov, D., Linhardt, R. J. & Mayo, K. H. (1996) *Biochem. J.* **315,** 447–454
44. Fromm, J. R., Hileman, R. E., Caldwell, E. E. O., Weiler, J. M. & Linhardt, R. J. (1995) *Arch. Biochem. Biophys.* **323,** 279–287
45. Mascotti, D. P. & Lohman, T. M. (1995) *Biochemistry* **34,** 2908–2915
46. Faham, S., Hileman, R. E., Fromm, J. R., Linhardt, R. J. & Rees, D. C. (1996) *Science* **271,** 1116–1120
47. Faham, S., Linhardt, R. J. & Rees, D. C. (1998) *Curr. Opin. Struct. Biol.* **8,** 578–586
48. Guimond, S., Maccarana, M., Olwin, B. B., Lindahl, U. & Rapraeger, A. C. (1993) *J. Biol. Chem.* **268,** 23906–23914
49. Ishihara, M., Karyia, Y., Kikuchi, H., Minamisawa, T. & Yoshida, K. (1997) *J. Biochem.* **121,** 345–349
50. Benton, R. E. & Gersh, B. J. (1998) *S. Med. J.* **91,** 133–137
51. Suh, J. S., Aster, R. H. & Visentin, G. P. (1998) *Blood* **3,** 916–922
52. Horne, M. K. & Hutchinson, K. J. (1998) *Am. J. Hematol.* **58,** 24–30
53. Visentin, G. P., Ford, S. E., Scott, J. P. & Aster, R. H. (1994) *J. Clin. Invest.* **93,** 81–88
54. Visentin, G. P., Malik, M., Cyganiak, K. A. & Aster, R. H. (1996) *J. Lab. Clin. Med.* **128,** 376- 385
55. Vemuri, S., Beylin, I., Sluzky, V., Stratton, P., Eberlein, G. & Wang, Y. I. (1994) *J. Pharm. Pharmacol.* **46,** 481–486
56. Chen, B. L. & Arakawa, T. (1996) *J. Pharm. Sci.* **85,** 419–426
57. Burke, C. J., Volkin, D. B., Mach, H. & Meddaugh, C. R. (1993) *Biochemistry* **32,** 6419–6425
58. Moy, F. J., Safran, M., Seddon, A. P., Kitchen, D., Bohlen, P., Aviezer, D., Yayon, A. & Powers, R. (1997) *Biochemistry* **36,** 4782–4791
59. Barnes, D. W., Reing, J. E. & Amos, B. (1985) *J. Biol. Chem.* **260,** 9117–9122